# Emission dynamics of reactive oxygen species and oxidative potential in particles from a gasoline car and wood stove

Battist Utinger[*,1], Alexandre Barth[*,1], Andreas Paul[2], Arya Mukherjee[3], Steven J. Campbell[4], Christa-Maria Müller[1], Mika Ihalainen[3], Pasi Yli-Pirilä[3], Miika Kortelainen[3], Zheng Fang[5], Patrick Martens[6,9], Markus Somero[3], Juho Louhisalmi[3], Thorsten Hohaus[2], Hendryk Czech[6,7], Olli Sippula[3,8], Yinon Rudich[5], Ralf Zimmermann[6,7], and Markus Kalberer[1]

[1]Department of Environmental Science, University of Basel, Basel, Switzerland
[2]IEK-8 Troposhere, Forschungszentrum Jülich GmbH, Jülich, Germany
[3]Department of Environmental and Biological Science, University of Eastern Finland, Kuopio, Finland
[4]MRC Centre for Environment and Health, Environmental Research Group, Imperial College London, London, UK
[5]Department of Earth and Planetary Science, Weizmann Institute of Science, Rehovot, Israel
[6]Department of Technical and Analytical Chemistry, University of Rostock, Rostock, Germany
[7]Cooperation group "Comprehensive Molecular Analytics", Helmholtz Centre Munich, Munich, Germany
[8]Department of Chemistry, University of Eastern Finland, Joensuu, Finland
[9]Now at: Desert Research Institute, 2215 Raggio Parkway, Reno, NV 89512, USA

*both authors equally contributed to the publication

*Correspondence to*: Markus Kalberer (markus.kalberer@unibas.ch)

**Abstract.** Air pollution is one of the largest environmental health risks and one of the leading causes of adverse health outcomes and mortality worldwide. The possible importance of the oxidative potential (OP) as a metric to quantify particle toxicity in air pollution is increasingly being recognized. In this work, the OP and reactive oxygen species (ROS) activity of particles from fresh and aged gasoline passenger car emissions and residential wood combustion (RWC) emissions were investigated using two novel instruments. Applying online instruments using an ascorbic acid (AA) and 2',7'-dichlorodihydrofluorescein (DCFH) assay provides a much higher time resolution compared to traditional filter-based methods and allows for new insights into highly dynamic changes in OP and ROS activity of these sources. Due to the efficiency of the particulate filter in the Euro 6d car, almost no primary particles were emitted and thus no particle OP and ROS was detected in primary exhaust. However, a substantial and highly dynamic OP and ROS activity was observed after photochemical ageing due to the formation of secondary particles. Increasing OP and ROS activity due to ageing was also observed when comparing fresh and aged RWC emissions. Overall, RWC emissions had ~~significantly~~ higher OP and ROS signals compared to car emissions. This suggests that aged RWC emissions could be a major contributor to air pollution toxicity, and may be an intrinsically more harmful emission source than car exhaust, although the formation potential for secondary particles from car emissions was still high. These measurements illustrate the strong differences and highly dynamic nature of toxicity-relevant particle properties from two air pollution sources and could contribute to more efficient air pollution mitigation policies.

## 1 Introduction

Air pollution is a complex mixture of gaseous compounds and aerosol particles composed of both natural and anthropogenic constituents, with common anthropogenic sources including fossil fuel combustion, non-exhaust traffic emissions, industrial processes, and agricultural activities. The specific composition and concentrations of pollutants in the ambient air varies depending on a range of factors like local sources and meteorological conditions. According to numerous epidemiological studies, there is a compelling association between air pollution and various health effects.(Hart et al., 2015; Laden et al., 2006; Lepeule et al., 2012) Elevated levels of ambient aerosol particles have been associated with increased hospital admissions and deaths from a variety of diseases, including cancer, respiratory illness, and cardiovascular disease.(Baulig et al., 2003; Donaldson et al., 2001; Li et al., 2003; Offer et al., 2022; Prahalad et al., 2001) The World Health Organization (WHO) recognizes in a recent report that air pollution and specifically aerosol particles are the single largest environmental threat to human health.(World Health Organization, 2021) Despite strong evidence linking air pollution particles and negative health outcomes, the specific mechanisms and properties by which aerosol particles cause these effects are poorly understood. Identifying the health-relevant particle properties, including the most damaging chemical components and their emission sources, will allow for the development of more effective strategies to minimize exposure from the most harmful sources.(Brunekreef and Holgate, 2002; Künzi et al., 2015) Current guidelines and legal regulations mainly address total particle mass concentration as the criterion to evaluate air quality. However, there is proof that differences in the chemical composition of particulate matter play a role in their toxicity.(Kelly and Fussell, 2012) There is increasing evidence that oxidising particle components might play a role in particle toxicity.(Øvrevik et al., 2015)

Reactive oxygen species (ROS) are highly reactive oxygen-containing molecules and radicals such as hydrogen peroxide, hydroxyl radical, superoxide, and organic peroxides and are formed in oxidation reactions in the atmosphere. These can be delivered exogenously through particle exposure (especially larger, less volatile organic peroxides and radicals) or can be produced endogenously when particles are deposited on the lung surface after inhalation such as hydroxyl radical or superoxide.(Campbell et al., 2019) Exogenous reactive species exist also in the gas phase, but in this study we focus on the particle exposure only. Another potential metric serving as proxy for particle toxicity is the oxidative potential (OP) of particles, which is defined as the ability of aerosol particle components to generate ROS inside the body ~~while~~ simultaneously depleting~~e~~ antioxidants.(Kelly, 2003) The exceedance of the body's anti-oxidative capacity can lead to oxidative stress which has been linked to negative health effects~~linked to causing negative health effects~~.(Pizzino et al., 2017) In recent years, the importance of OP and ROS in air pollution research has gained increasing attention as these parameters might play a major role in PM-induced diseases.(Guascito et al., 2023) For example, the European parliament recently adopted a revised Ambient Air Quality Directive for Europe.(European Parliament, 2024) It suggests the expansion of monitored pollutants at supersites to also include OP among other pollutants of emerging concern next to the standard network of measurements.(European Union, 2022)

Usually, ROS and OP measurements have been based on the collection of PM filters and subsequent laboratory analysis. However, the time lag between sample collection and analysis can be long, potentially leading to a severe underestimation of PM OP due to the instability and therefore short lifetime of ROS. Recent studies showed that only a minor fraction (1-40%) of particle-bound ROS in organic aerosol collected on filters is stable on a time scale of up to a week compared to direct-to-reagent online measurements, emphasizing the need for immediate analysis of particles for accurate quantification of ROS and OP.(Campbell et al., 2023; Zhang et al., 2021) Other studies have also shown short half-lives of compounds contributing to ROS and OP in aerosol particles such as radicals (Campbell et al., 2019), peroxy acids (Steimer et al., 2018), and hydroperoxides (Zhao et al., 2018) ranging from minutes to hours. These findings indicate that online measurement methods that utilise a direct-to-reagent sampling approach are required for robust quantification of OP and ROS, particularly to capture the short-lived reactive components.

PM originating from anthropogenic sources typically has higher OP than natural emissions, as evidenced by a recent study which observed a factor of three higher OP for anthropogenic compared to biogenic secondary organic aerosol (SOA).(Daellenbach et al., 2020; Zhang et al., 2021) Two important classes of anthropogenic aerosols are emissions from residential wood combustion (RWC) and traffic emissions. The anthropogenic contribution from RWC is especially visible during winter, when most of $PM_{2.5}$ comes from biomass burning. (Gon et al., 2014) Even at very low ambient concentrations of PM attributed to residential wood combustion, there is an observable health impact. A recent study estimated that annual concentrations of RWC aerosol as low as 0.46 $\mu g/m^3$ can lead to a decrease in life expectancy of 0.1 years.(Orru et al., 2022) Additionally, emissions from road traffic are a major source of urban air pollution. While modern exhaust treatment systems can reduce primary emissions of PM, the formation potential of secondary emissions is still high, even with engines complying to the newest regulations. (Gao et al., 2021; Hartikainen et al., 2023; Platt et al., 2017)

Recent studies have attempted to uncover the relationship between composition and potential biological ~~health~~ effects of PM.(Campbell et al., 2024) OP has emerged as a novel and biologically significant chemical metric that may serve as a critical connection between the chemical composition of particles and their associated adverse health effects.(Bates et al., 2019) Specific components like organic/elemental carbon and metals were associated with an increased risk of negative health outcomes.(Atkinson et al., 2015; Heo et al., 2014) Thus, the composition of aerosol particles and their emission sources play a key role in dictating OP and ROS formation. Determining the sources and components which influence OP in the complex ambient aerosol is poorly understood but would provide~~s~~ cruciFin real information for policymakers to more efficiently abate air pollution.

In this study we ~~close the~~address this knowledge gap ~~of measuring,~~and quantify for the first time the highly dynamic particulate OP and ROS characteristics of emissions of ~~a~~ gasoline passenger car as well as of a ~~a~~ residential wood stove ~~emissions were investigated.~~ Two recently developed online instruments were used in this study, which allow for unprecedented high time resolution (10 min) OP and ROS measurements ~~were deployed~~: the online oxidative potential ascorbic acid instrument

(OOPAAI) measures aerosol particle OP using an online ascorbic acid assay ~~as described by Utinger et al., 2023~~ (Utinger et al., 2023) and the online particle-bound ROS instrument (OPROSI) quantifies particle-bound ROS.(Wragg et al., 2016) Besides sampling the emissions directly (i.e. primary emissions) they were also passed through a photochemical flow tube reactor to simulate two different atmospheric ageing conditions. ~~-~~Combustion conditions have highly dynamic emissions profiles and only online instruments, as used in this study, are able to characterise fast-changing OP- and ROS properties of particle emissions. Furthermore, we calculated for the first time emission factors for OP ($EF_{OP}$) and ROS ($EF_{ROS}$) enabling the assessment of health risks ~~potentially allowing to assess health risks~~ associated with exposure to PM emitted from these two sources and to provide information on a potential link between atmospheric ageing of particles and oxidative stress.

## 2 Material and Methods

### 2.1 Reagents

All chemicals were obtained from Sigma-Aldrich and were used without further purification unless otherwise indicated: ascorbic acid (AA, 99.0%), d~~D~~ehydroascorbic acid (DHA, 99.0%), hydrochloric acid ~~0.1 M~~ (HCl~~L~~, 0.1 M) sodium hydroxide ~~0.1 M~~ (NaOH, 0.1 M) solution, Chelex 100 sodium form, o-phenylenediamine (OPDA, ≥99.5%), ~~HEPES~~ (4-(2-hydroxyethyl)-1-piperazineethanesulfonic acid (HEPES, ≥ 99%), methanol (99.9%), peroxidase from horseradish (Type VI, HRP), ~~DCFH-DA~~ (2,7-Dichlorofluorescin diacetate ~~,~~ (DCFH-DA, 97%), 3% hydrogen peroxide solution, ~~1 M~~ phosphate-buffered saline solution (PBS, 1M) ~~solution~~, zero grade air (Model 737–250, Aadco Instruments Inc., USA), $N_2$ gas (~~purity~~ 99.999%, Linde, Finland).

## 2.2 Aerosol Generation and Characterization

Here, only a brief overview of the experimental setup of emission generation and ageing, as well as sampling, is given. More details can be found in Mukherjee et al., 2024, and Paul et al., 2024.(Mukherjee et al., 2024; Paul et al., 2024) Figure 1 illustrates a simplified schematic of the experimental setup. The raw exhaust was sampled directly at the tail pipe of a EURO 6d gasoline car (Škoda Scala 2021) or the chimney of a residential wood stove (Aduro 9.3). Flowing through a heated sampling line, a two-step dilution system reduced the concentration and temperature of the sample using a porous tube and an ejection

diluter. The dilution ratio was set at 1:17 during the car emission experiments and 1:60 during the RWC experiments because

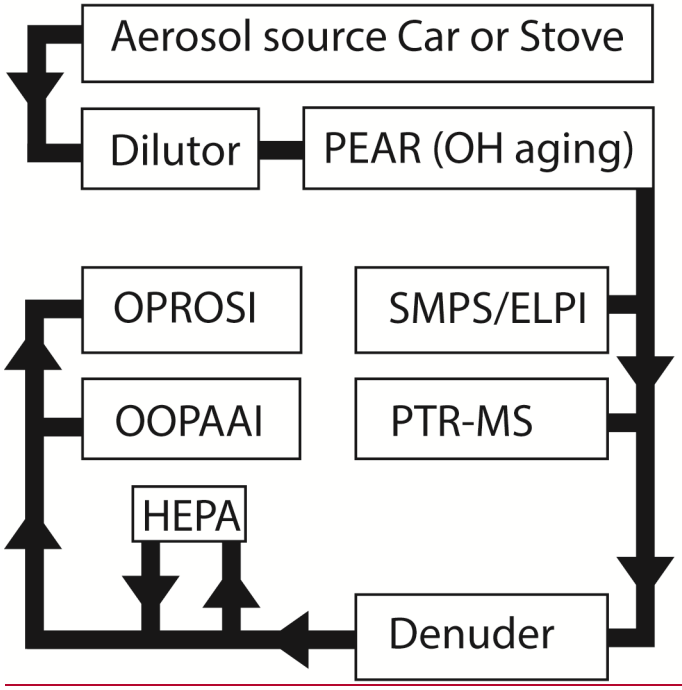


**Figure 1A simplified schematic of the components and analysis instruments relevant for this paper. The aerosol is transported and diluted from the emission source to the PEAR chamber and after further dilution and removal of reactive gas-phase componen**

of the large difference in PM and gas phase concentrations of the two PM sources and to assure a final maximal PM concentration between 500 and 2000 µg/m$^3$ (Fig. 2 and 5). The exhaust flow then passed through the photochemical emission ageing flow tube reactor (PEAR) to simulate atmospheric ageing.(Ihalainen et al., 2019) For primary experiments the PEAR was not in operation, but the aerosol was passed through it nonetheless to have comparable results. The equivalent photochemical ages were determined to be between 1.1 and 5.1 days ~~using~~ by determining the decay kinetics of fully deuterated butanol measured by a proton-transfer-reaction time-of-flight mass spectrometer (PTR-TOFMS 8000, ~~Iconic~~Ionicon).(Paul et al., 2024; Schneider et al., 2024). Furthermore, a scanning mobility particle sizer (SMPS,~~-~~ Model 3776 CPC, Model 3080 classifier, TSI) and a low-pressure impactor mass measurements (ELPI, Dekati) were used to quantify the particle number size distributions. The OOPAAI and OPROSI were connected after the PEAR to measure OP and ROS from both primary and secondary emissions.~~to measure both primary and secondary emissions.~~ Primary emissions without oxidative ageing by the PEAR were measured as well, to allow for the comparison between primary and aged combustion particles. Due to high particle concentrations during the RWC experiments, an additional porous tube diluter was connected and set to a dilution ratio of 1:1.5 to 1:3, depending on experimental conditions. By passing the sample through a high efficiency particle arresting (HEPA) filter (HEPA-CAP150, Whatman), blank measurements were possible during experiments to check for background drifts or

gas-phase artefacts. Subsequently, two 1 m long home-built denuders filled with activated charcoal (untreated, granular, Sigma-Aldrich) as well as one denuder with 8 honey-comb shaped charcoal elements (Ionicon) were connected in-line to remove any reactive gas-phase components that could contribute to the online ROS or OP signals (e.g., $O_3$ or oxidizing volatile organic compounds). The charcoal was regenerated at 230 °C for 24 h every second day. Having both instruments connected to the same denuders allowed for a higher sample flow through them, reducing particle losses, which were estimated to be 10% and the data was corrected by that value (Figure S 1).

The car was operated following a driving cycle, where one cycle lasted for an hour and an experiment consisted of four cycles equalling to 4-hour measurement periods. Every cycle consisted of four different steady-state driving conditions starting with 5 min of idling, followed by each 15 min of 50 km/h (4$^{th}$ gear), 100 km/h (5$^{th}$ gear), 80 km/h (5$^{th}$ gear) and ending with 10 minutes of idling. For the RWC measurements, an initial batch of beech wood logs (1.85 kg) with 150 g of beech kindling was ignited. Similar procedures were used in other studies using the same stove.(Ihantola et al., 2022; Leskinen et al., 2023; Martens et al., 2021) After every 35 min an additional batch of 2 kg of beech logs was added for a total of six batches. After the last addition, the wood was left to burn out (ember phase) for 30 min during which the supply of fresh air was stopped. One RWC experiment lasted 4 h. Blank OP and ROS measurements were performed before and after experiments as well as at different time points during an experiment to characterize potential gas-phase contributions, denuder efficiency, and instrument backgrounds. The OOPAAI was started the day before an experiment day and blank measurements were run overnight to assure a stable blank. The OPROSI was started only ~~at least~~ one hour before the start of an experiment due to higher costs for chemicals and a faster stable blank. The cellulose grade 1 filters inside the liquid systems of both instruments, which remove insoluble particles were changed daily to avoid excessive contamination by insoluble particles (see section 3.2 for further details). Additionally, this was done between each 4 h run of the RWC experiments for the OPROSI. The OOPAAI and OPROSI were calibrated once a week to ensure consistent performance for the duration of the measurement campaign.~~.~~ ~~Otherwise, they were operated~~ as described in Wragg et al., 2016 (Wragg et al., 2016) and Utinger et al., 2023.(Utinger et al., 2023)

### 2.3 Chemical Preparation

All chemical solutions used in this study were made immediately prior to measurements, except where otherwise specified. Water used to prepare the solutions was purified by a high purification water unit (resistivity 18.2 MΩ/cm). For the ascorbic acid assay the water ~~To further reduce the amount of contamination, water~~ was passed through a fritted column filled with 100 g Chelex 100 resin, to further reduce the amount of contamination. The valve was adjusted to a flow of one drop per minute through the resin. The treatment was used to remove trace metals (i.e. copper and iron) to avoid interference with the AA oxidation caused by the sample. A 200 mM HEPES buffer stock solution to adjust the pH to a physiological relevant range (pH 6.8) was prepared monthly using Chelex treated water and stored at 4 °C. HEPES was used because it has a lower chelating effect of transition metals than PBS.(Utinger et al., 2023) AA solutions were prepared the day before the experiments in an effort to stabilize the background drift caused by the autooxidation of AA. 8.8 mg of AA were dissolved in 25 mL HEPES

stock solution and 225 mL Chelex treated water to form a 200 µM AA working solution. OPDA solution was prepared by dissolving 0.54 g in 250 mL of 0.1 M hydrochloric acid to form a 20 mM working solution. For the ROS measurements of the DCFH assay the HRP stock solution was prepared weekly by dissolving 5000 units in 500 mL of water and stored at 4 °C. HRP working solution was prepared using 100 mL of HRP stock solution, 100 mL of 1 M PBS, and 800 mL of pure water. DCFH-DA stock solution was prepared weekly by dissolving 50 mg of DCFH-DA in 50 mL of methanol and sonicating it for 15 s and stored at −20 °C. DCFH working solution was prepared by reacting 4 mL 0.1 M NaOH with 4.872 mL of the DCFH-DA stock solution for 30 min in the dark. Subsequently, 100 mL of 1 M PBS and pure water were added to a total volume of 1 L. The HRP and DCFH working solutions were prepared the night before and stored at 4 °C. For both assays a calibration was performed once per week as described in Utinger et al., 2023 for ascorbic acid and Wragg et al., 2016 for DCFH to convert the raw fluorescence signal to the corresponding equivalents using known concentrations of DHA and $H_2O_2$. (Utinger et al., 2023; Wragg et al., 2016)

### 2.4 Data Analysis

The fluorescence spectroscopy data was first corrected for the blank background and its drift over the four-hour measurement period. This was done by applying a fit across all blank measurements and subtracting the fitted blank values from the raw signal. The drift was less pronounced in the OOPAAI for the car exhaust measurements and a linear fit was sufficient. However, for the stronger drifts during the RWC measurements, the baseline was fitted using a B-spline function in OriginPRO (OriginLab 2023). For the OPROSI corrections, a polynomial fit of 3$^{rd}$ order was used for the car and RWC data. The data were averaged to 10 s to match the electrical low-pressure impactor mass measurements (ELPI, Dekati) providing total $PM_{2.5}$ mass concentrations. The ELPI particle size range used for the car measurements was $PM_{0.3}$ while $PM_{0.6}$ was used for the RWC emissions. These size ranges were chosen because gaseous ions in the exhaust gas would lead to measurement artefacts and a considerable overestimation of total PM mass in the larger size bins of the ELPI. This can be shown as no significant particle concentrations were present above these size ranges as measured by the SMPS as well as ELPI (Figure S 23). (Paul et al., 2024) Taking these ELPI size bins, the mass concentrations were in a similar range as measured by the SMPS while still offering a higher time resolution (Figure S 34). A constant particle density of 1.6 g/cm$^3$ was used for mass calculations of the car measurements (Paul et al., 2024) and for PM emitted by the stove densities from Mukherjee et al., 2024, were used (Mukherjee et al., 2024). Average values of PM densities of 1.5, 1.75, and 1.85 g/cm$^3$ during the flaming and residual burning phases were used for fresh, short aged, and medium-aged measurements, respectively. The methods to derive ROS and OP emission factors (EF) for car exhaust and for RWC PM are described and derived in Paul et al., 2024, and Reda et al., 2015, respectively. (Paul et al., 2024; Reda et al., 2015) and calculated as shown in the following equation:

$$EF = \frac{nmol\ ROS}{kg\ fuel} = \frac{mg\ aerosol}{kg\ fuel}\ x\ \frac{nmol\ ROS}{mg\ aerosol}$$

## 3 Results and Discussion

OP and ROS concentrations of tail pipe particle emissions from a EURO 6d gasoline car as well as from beech wood combustion using a residential wood stove were quantified. Fresh emissions were characterised but also changes in chemical properties were studied caused by photochemical ageing in a flow tube reactor. The OP and ROS results are presented normalized to the sampled air volume ($OP_V$ and $ROS_V$) as well as normalized to PM mass ($OP_M$ and $ROS_M$).

### 3.1 OP and ROS concentrations of Primary and Secondary Car Exhaust Emissions

Four-hour experiments were performed and consisted of four one hour driving cycles with an idling phase and three engine loads as described in the method section.

Both instruments could not detect any signal for the primary exhaust (Figure S 4~~5~~). As part of the EURO 6d regulations, the car's exhaust system is fitted with a gasoline particle filter (GPF) reducing primary exhaust emissions.(Paul et al., 2024) Thus, possible particle OP and ROS activity in primary particulate emission were below the detection limit of our online instruments. LODs (in units of nmol DHA $m^{-3}$ and nmol $H_2O_2$ $m^{-3}$, respectively) depend on the OP and ROS content of the respective particle and is therefore variable. For SOA, LOD is around 5ug/m3 ((Utinger et al., 2023; Wragg et al., 2016)) which is much lower than any of the conditions measured during this campaign where no GFP was used. In contrast, as illustrated in Figure 2~~Figure 2~~, significant $OP_V$ and $ROS_V$ ~~concentrations~~ values and particle mass ($PM_{2.5}$) were measured for photochemically aged car exhaust for an equivalent atmospheric ageing of 2.1 days in the PEAR chamber with OP and ROS concentrations of up to 800 nmol DHA $m^{-3}$ and 2200 nmol $H_2O_2$ equivalents $m^{-3}$ were measured. Aged particle emissions consisted only of secondary organic and inorganic particles. Figure 2 clearly demonstrates that both instruments are sensitive to SOA, as also shown in previous studies (Utinger et al., 2023; Wragg et al., 2016) while inorganic secondary particles, mainly composed of $NH_4$, $SO_4$ and $NO_3$, do not react with the AA and DCFH in our online instruments.(Paul et al., 2024) $OP_V$ and $ROS_V$ concentrations generally follow the particle mass closely, although some changes in PM mass are not reflected in $OP_V$ and $ROS_V$. This shows that different engine loads not only cause a change in total aged PM mass concentration, but also in particle OP and ROS activity. The highest mass concentrations and also OP and ROS signals ~~is~~were measured at 50 km/h compared to 80 km/h and 100 km/h were lower OP, ROS and mass concentrations were observed. During the last cycle (Figure 2, after 03:00), blank OP and ROS measurements were performed by removing all particles from the exhaust flow with a HEPA filter in front of the OOPAAI and OPROSI. These blank measurements clearly illustrate that gaseous components in the aged exhaust were removed efficiently by the charcoal denuders

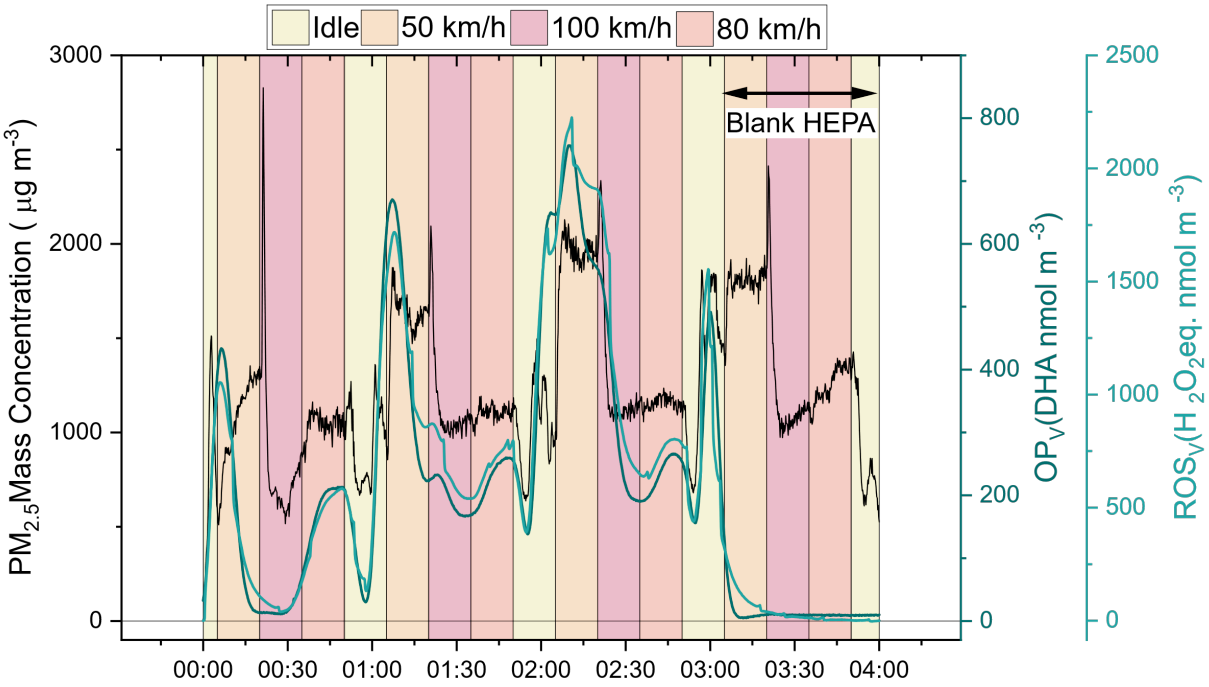


**Figure 2: $OP_V$ and $ROS_V$ measurement of secondary car emissions after an equivalent of 2.1 days aging during four driving cycles as well as the particle mass measured by an ELPI. $OP_V$ and $ROS_V$ are given in nmol DHA/m$^3$ and nmol $H_2O_2$ eq./m$^3$, respectively. The last hour of measurements after 03:00 was used for a HEPA blank, removing all particles from the sample flow.**

in our instruments (Figure 1) and do not cause any measurement artefacts, since both instruments returned to blank-level values.

Two different ageing conditions were applied to investigate the potential influence of photochemical ageing on the intrinsic OP and ROS. In Figure 3~~Figure 3~~ the averaged $OP_M$ of the two ageing conditions are shown. Photochemical ages of approximately 2.1 days (Figure 3~~Figure 3~~A) and 5.1 days (Figure 3~~Figure 3~~B) represent short and medium ageing processes in the atmosphere. Overall, the $OP_M$ was similar between the two ageing times. We observed about two times higher peak $OP_M$ concentrations during idling and at the beginning of the 50 km/h period compared to the other engine conditions with 100 and 80 km/h loads during the short ageing condition (0.31 ± 0.19 nmol DHA µg$^{-1}$ vs. 0.15 ± 0.03 nmol DHA µg$^{-1}$). This difference was larger by about 40% during the medium ageing condition (0.41 ± 0.29 nmol DHA µg$^{-1}$ vs. 0.12 ± 0.08 nmol DHA µg$^{-1}$). The idling and 50 km/h periods also show the highest variability across all averaged 15 driving cycles due to fluctuations of the emissions. Interestingly, a consistent short increase in $OP_M$ of 65% at the beginning of the 100 km/h condition was measured (at about 00:25). This could be due to the strong acceleration of the engine similarly to the transition from idle to 50 km/h, causing non-ideal combustion conditions.

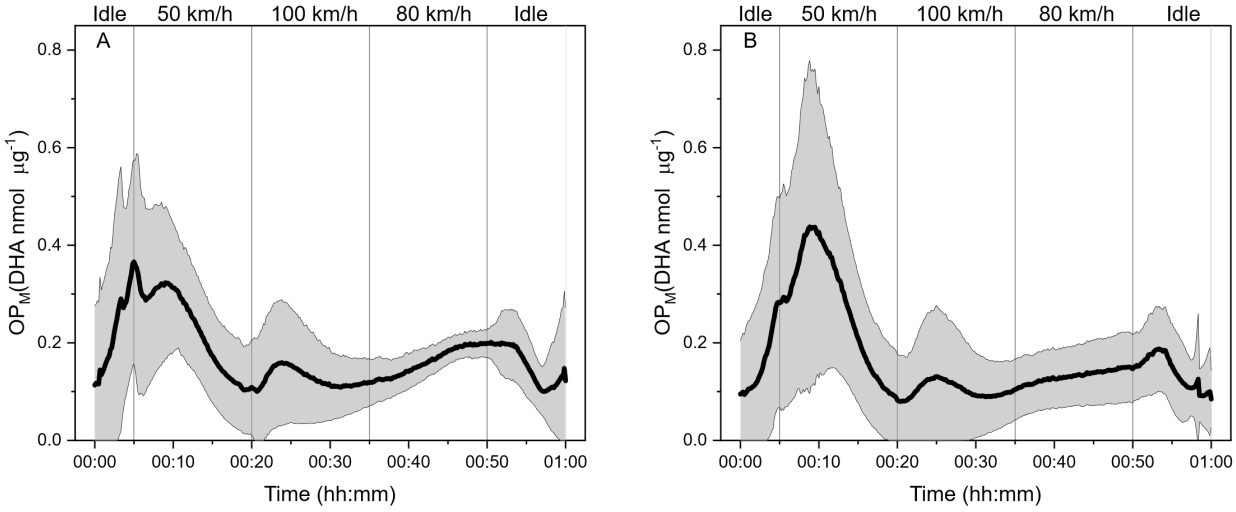


**Figure 3: $OP_M$ concentrations after 2.1 days (A) and 5.1 days (B) photochemical ageing of car emissions. The average of 15 driving cycles is represented in one cycle (black line). The error band (grey shaded area) shown is the standard deviation of the 15 driving cycles.**

The $ROS_M$ concentrations of the two photochemical ageing conditions are shown in Figure 4~~Figure 4~~. Overall, ROS behaviour was similar to the $OP_M$ results across all driving conditions with 40% higher $ROS_M$ values observed during the transition from idle to 50 km/h compared the concentrations measured during 100 and 80 km/h periods and the same slight and transient increase of approximately 30% at the beginning of the 100 km/h (00:25) condition was observed. Unlike the $OP_M$, the $ROS_M$ signal decreased with aging and was 30-70% higher during short ageing (Figure 4~~Figure 4~~A) compared to the medium ageing (Figure 4~~Figure 4~~B) across all driving conditions. A possible explanation for this decrease of ROS with increasing ageing time could be photolytic decomposition of peroxides over time. Other studies using an atmospheric simulation chamber also observed a decrease in ROS activity with longer photochemical ages (several hours to days) for two-stroke scooter engine emissions as well as biogenic SOA.(Epstein et al., 2014; Platt et al., 2014)

The OP and ROS activity during cold starts at the beginning of an experiment is not distinguishable from following driving cycles (warm start) during a four-hour experiment. Because ~~this period is~~ the cold start is very short (5 min) and thus within the time resolution of both the OOPAAI and OPROSI instruments, the difference from cold start could not be resolved ~~potential effect would be difficult to resolve.~~ and therefore it was not analyzed separately.

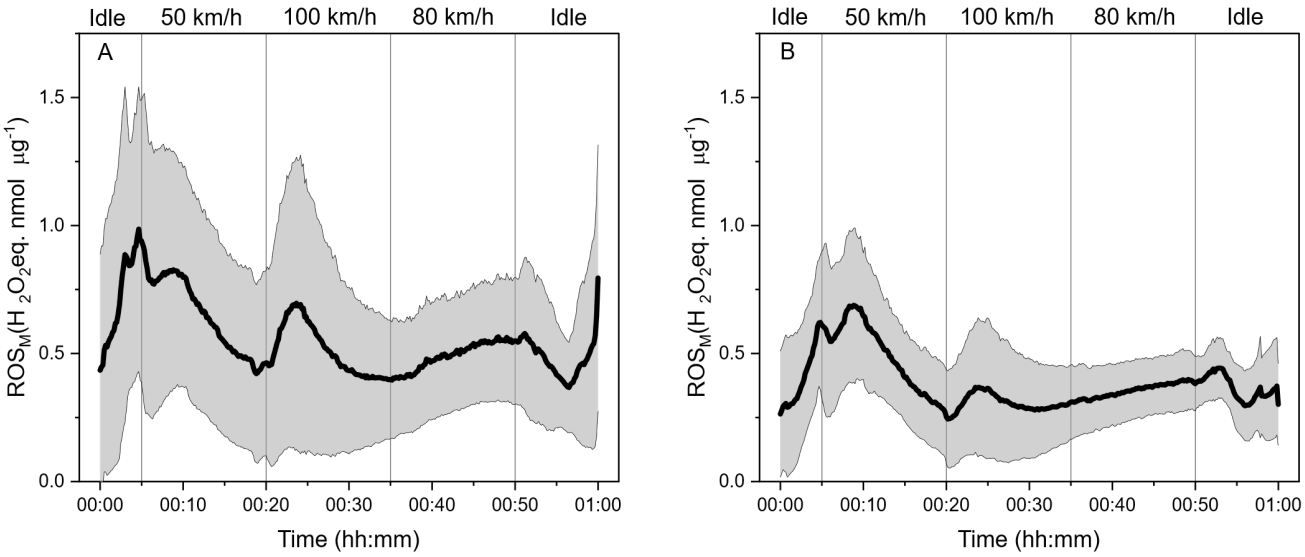


**Figure 4: $ROS_M$ concentration of 2.1 days (A) and 5.1 days (B) in aged car emissions. The average of 15 driving cycles for short ageing and medium ageing is represented in one cycle (black line). The error band (grey shaded area) shown is the standard deviation of the 15 driving cycles.**

### 3.2 OP and ROS Concentrations from Residential Wood Combustion (RWC) Particles

For the RWC experiments, primary emissions as well as two ageing conditions were investigated. In Figure 5~~Figure 5~~ $OP_V$ and $ROS_V$ measurements are shown as well as the particle mass measured by an ELPI during a four-hour experiment with RWC aged for an equivalent of up to 3.3 days. Light and darker blue background colours indicate the addition of a new wood batch (see method section). The last batch was left to burn for additional 30 min as ember phase (yellow background).

Both instruments observed an increase and subsequently a decrease in $OP_V$ and $ROS_V$, respectively, with each batch. $OP_V$ and $ROS_V$ reached peak values in the first half of a 35 min long batch with approximately a factor of ten higher compared to values at the end of a batch. This again demonstrates how both online instruments are capable of capturing fast changing emission characteristics. After six batches of ~~RWC~~ wood added to the stove, the ember phase started, characterised by low emissions of $OP_V$ and $ROS_V$ as well as particles~~characterised by low particulate emissions. The $OP_V$ and $ROS_V$ signals gradually decreased accordingly to zero, because there is no particulate emission~~. Compared to the car experiments, the RWC results showed a higher batch-to-batch variability, observed by both instruments as well as the particle mass concentration which was also reported in previous RWC studies.(Heringa et al., 2012; Vicente et al., 2015)

In contrast to the car emissions where no primary particles were emitted due to the GPF, both instruments responded to the primary RWC emissions~~. due to the significantly higher primary PM emissions~~. The OOPAAI observed an $OP_v$ signal for primary emission which was up to three times lower than during the aged experiments (Figure S6), which can be expected as ROS are predominantly formed through oxidation processes.

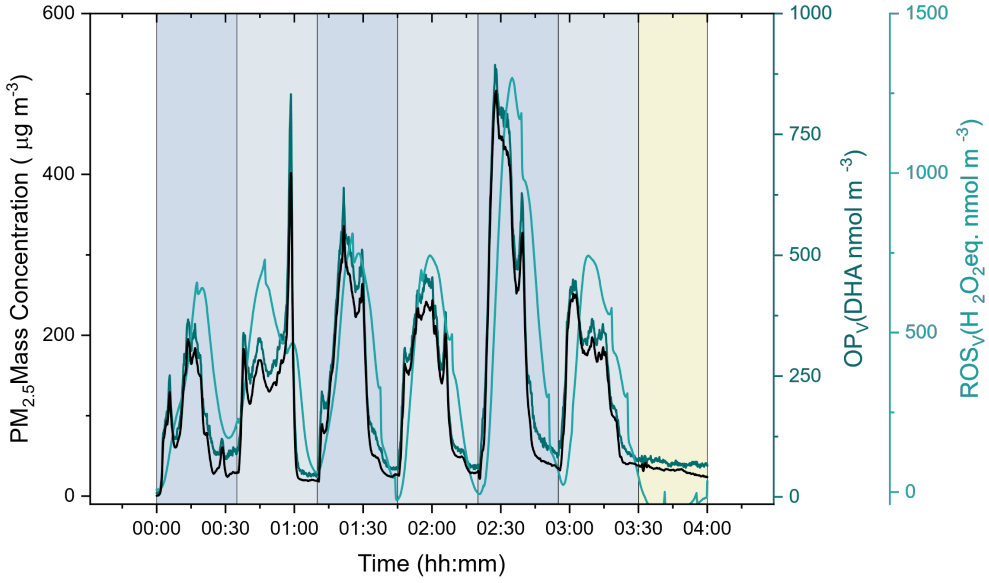


**Figure 5: $OP_V$ (dark green) and $ROS_V$ (light green) measurement of one secondary RWC emissions experiment as well as the particle mass (left axis, black line) measured by an ELPI. The blue boxes mark the different batches of wood added to the oven and the yellow box the ember phase.**

In contrast, the OPROSI showed a different response to primary RWC particles with negative ROS values (Figure S 5~~6~~), which might be a measurement artefact of the large fraction of insoluble primary PM (e.g. soot). Due to the high PM and specifically soot concentrations during these emission measurements, particles accumulated inside the instruments and potentially interacted with and deactivated the assay, causing the ROS signal to fall below blank values. The hydrophobic and large surface area of the soot particles could adsorb and inactivate reagents of the assay (e.g. HRP), causing an apparent lower ROS concentration compared to the blank. Enzymes are known to change their activity due to absorption onto a high surface area substrate.(Khan, 2021) To test this hypothesis in a qualitative way, activated charcoal was mixed with the ROS assay as a proxy for soot since it has also a high hydrophobic surface area. Figure S 6~~2~~ shows a clear decrease of the ROS signal with higher concentrations of charcoal~~. Unfortunately, thi~~, which~~s~~ is a fundamental limitation of the DCFH assay at very high insoluble particle concentrations ~~that is adding to the uncertainty of the measurement~~. Organic components in the primary particles, e.g. antioxidant compounds frequently found in wood smoke such as phenols, could also cause a signal decrease by reacting with HRP.(Kjällstrand and Petersson, 2001) The negative ROS peaks were less than 10% of the positive signals for

the aged exhaust and thus any uncertainties of aged ROS values related to the very high soot or antioxidant conditions are likely in the same range.

~~Photochemical ageing led to a significant increase of the $OP_M$ and $ROS_M$ activity compared to fresh emissions (Figure 6), while the PM mass range stayed within the same order of magnitude as during the primary measurements.~~ In Figure 6~~Figure 6~~, the $OP_M$ of the primary aerosol and the two ageing conditions are shown with the standard deviation from 16-21 repeat measurements. Two different ageing conditions with 1.4 ± 0.2 (short) and 3.3 ± 0.4 days (medium) were investigated. The ember phase is not considered in these figures since it did not show any detectable OP or ROS activity (data not shown). The primary aerosol (Figure 6~~Figure 6~~A) resulted in low (between 0 and 2 DHA nmol $\mu g^{-1}$) and stable $OP_M$ values in the same range as the car emissions for the majority of a batch. Near the end, when the wood was almost burned up and when no flames were visible anymore in some cases, $OP_M$ increased sharply by up to a factor of 6 compared to the rest of the batch. A continuous increase was observed during the short ageing condition with peak values being reached in the last 10 minutes of a batch (Figure 6~~Figure 6~~B). For the short agein t~~T~~he average $OP_M$ values remained comparable to the primary aerosol during the same time period within a large batch-to-batch variability (5.19 ± 9.48 nmol DHA $\mu g^{-1}$ vs. 6.48 ± 8.30 nmol DHA $\mu g^{-1}$). For medium ageing condition, t~~T~~he large increase in $OP_M$ at the end of a batch (as seen for primary emissions and short aging) was no longer observed while $OP_M$ concentrations still increased continuously during the course of a batch, similar to short aging conditions (Figure 6~~Figure 6~~B~~C~~). This resulted in an overall lower $OP_M$ with medium ageing.

The reduction of $OP_M$ from short to medium ageing could be due to chemical changes of PM components caused by prolonged oxidation reactions. For example, the oxidation of PAHs in the atmosphere, formed during wood combustion, can lead to the formation of quinone-type products, (Walgraeve et al., 2010) which are known to produce ROS in an aqueous solution and therefore would also contribute to OP in the OOPAAI.(Charrier and Anastasio, 2012; Li et al., 2003; Njus et al., 2023).

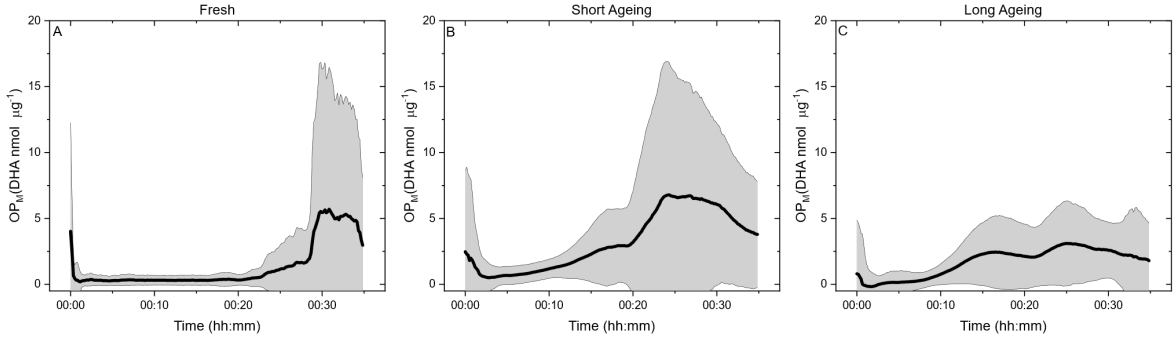


**Figure 6: Average $OP_M$ of ~~0~~ days (fresh, 21 batches, A), 1.4 ± 0.2 days (short, 16 batches, B) and 3.3 ± 0.4 days (medium, 17 batches C) RWC emissions (black line). The error showed is the standard deviation of the averaged batches (grey shaded area).**

However, continued oxidation during medium ageing may result in further oxidation of such OP-active quinones into inactive compounds, which would result in a lower OP activity. This effect has been observed for markers of biomass-burning SOA before through the breakdown of aromatic rings.(Fang et al., 2024) Wong et al. observed an overall decrease of OP in aged

laboratory-generated biomass burning aerosol after a short initial increase similar to our OP measurements with ascorbic acid.(Wong et al., 2019) This overall decrease with higher ageing could also partially be explained by the decrease in quinone concentrations in wood smoke observed with higher ages.(Jiang and Jang, 2018) Also for certain SOA types from gaseous precursors β-pinene and naphthalene, it was observed that using the DCFH assay more ageing does not induce a higher OP.(Offer et al., 2022). ~~Figure 7~~ shows the $ROS_M$ values for the two ageing conditions. For the primary RWC aerosol ROS signals could not be determined as discussed above. Similar to $OP_M$, the highest $ROS_M$ values were observed in later parts of a batch during both ageing conditions. However, this trend was more pronounced during the medium ageing experiments, in contrast to $OP_M$. $ROS_M$ during short ageing (Figure 7A) was three times lower compared to the medium ageing results (Figure 7B). More oxidized aerosol is generally associated with more oxygenated fraction of PM such as peroxides. To which the DCFH assay is especially sensitive.(Fang et al., 2024; Li et al., 2021; Nordin et al., 2015; Wang et al., 2023; Zhang et al., 2021) This is in agreement with aging of wood smoke in an atmospheric simulation chamber, where ageing by OH also lead to an increase in ROS activity.(Wang et al., 2023) Zhang et al. (2021) also measured an increase in ROS with higher ageing times for two simple SOA systems using β-pinene and naphthalene as precursors.(Zhang et al., 2021)

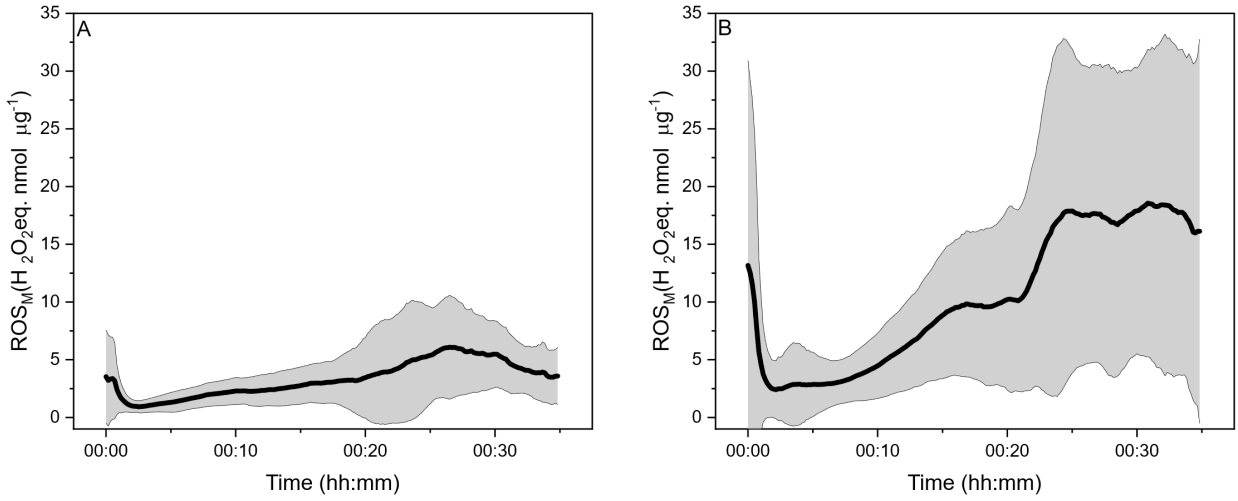


**Figure 7: Average $ROS_M$ concentrations for 1.4 ± 0.2 days (short, A~~B~~, 16 batches) and 3.3 ± 0.4 days (medium, B~~C~~, 17 batches) RWC emissions (black line). The standard deviation of the different measurements is plotted as an error band (grey shaded area).**

### 3.3 Comparison of $OP_M$ and $ROS_M$ and Emission Factors of Car Exhaust and RWC

Table 1~~Table 1~~ summarizes the $OP_M$ and $ROS_M$ values we observed covering a realistic range of atmospheric oxidative processing times up to 5 days. The $OP_M$ and $ROS_M$ activity measured during this study were highly dynamic, changing up to two orders of magnitude within minutes and are comparable to other lab studies characterising pure SOA systems conducted with similar online instruments.(Campbell et al., 2023; Zhang et al., 2021)

**Table 1: Overview of the measured $OP_M$ and $ROS_M$ values illustrating the large range observed within a cycle (car) or batch (RWC) as a result of the high-time-resolution online measurements. To determine the atmospheric age (in days) for the RWC measurements the average and standard deviation of 5 ageing condition measurements is given, while for the car exhaust only one measurement per age was conducted.**

| Source | Age (days) | $OP_M$ (nmol DHA $\mu g^{-1}$) | $ROS_M$ (nmol $H_2O_2$ eq. $\mu g^{-1}$) |
|---|---|---|---|
| Car | 0.0 | N/A | N/A |
| | 2.1 | 0.1-0.4 | 0.4-1.0 |
| | 5.1 | 0.1-0.4 | 0.2-0.7 |
| RWC | 0.0 | 0.2-5.7 | N/A |
| | 1.4 ± 0.2 | 0.5-6.8 | 0.9-6.1 |
| | 3.3 ± 0.4 | 0.0-3.1 | 2.4-18.6 |

A comparison of primary particles is not possible, because the car has a GPF and therefore almost no primary particle emissions, in contrast to the stove with ~~significantly~~ more primary particles. This means that during the stove experiments combined effects of primary and secondary aerosols on the OP and ROS activity were observed while only secondary car particles were measured. The lack of primary particles could partially be responsible for the up to one order of magnitude higher $OP_M$ and $ROS_M$ values from the wood stove. The large difference in $OP_M$ and $ROS_M$ between car and RWC emissions could also be explained by the difference in composition of the secondary particles. A ~~significant~~ compositional difference is the metal content of the two aerosol types. Wood smoke is known to contain a wide range of redox active metals, including zinc, iron and copper.(Erlandsson et al., 2020; Gonçalves et al., 2010; Uski et al., 2015) The total metal concentrations can reach up to 2.5 wt.% of $PM_{2.5}$ depending on wood type and combustion appliance whereas car exhaust treated with a particulate filter only contains very low concentration of metallic primary particles and consists mostly of secondary aerosol.(Alves et al., 2011) The presence of transition metals has been shown to have an influence on the OP and ROS activity of SOA. Campbell et al. observed synergistic effects leading to higher $OP_M$ when biogenic SOA and metals are combined.(Campbell et al., 2023) In addition, differences in SOA composition from these two sources are likely also contributing to the observed differences in $OP_M$ and $ROS_M$.

Emission factors are calculated and used to estimate the quantity of pollutants released into the atmosphere from various sources, helping to assess environmental impacts and guide regulatory compliance and mitigation efforts. To the best of our knowledge, emission factors of OP and ROS have never been reported in the literature before. Figure ~~Figure 8~~A shows $EF_{OP}$

and $EF_{ROS}$ for different driving speeds and both ageing conditions in pmol DHA/kg fuel and pmol $H_2O_2$ eq./kg fuel, respectively. Similar to the PM mass normalized OP and ROS results, the 50 km/h condition resulted in the highest EF values. Medium ageing led to an overall increase of $EF_{OP}$ and $EF_{ROS}$. The smallest change was observed for a speed of 100 km/h. Figure ~~Figure 8~~B shows emission factors for RWC for fresh emissions, as well as short and medium ageing. Opposite effects of ageing on the two assays are visible similar to trends in the mass-normalised $OP_M$ and $ROS_M$ data (Fig. 6 and 7): An increase in ageing leads to a reduction of $EF_{OP}$ but to an increase of $EF_{ROS}$. No ~~significant difference~~clear trend in $EF_{ROSOP}$ ~~e~~between the two ~~emparing both~~ aging conditions (blue, short aging and blue stripes, medium aging for the car and short and medium for RWC) was detected. ~~due to the variability between the different repeat experiments~~$EF_{OP}$ ~~of both aging conditions (blue, short aging and blue stripes, medium aging for the car and short and medium for RWC) are in error of the variability for~~very ~~similar for both sources and therefore no difference could be seen. For~~ $EF_{ROS}$ and $EF_{OP}$ for gasoline car emissions are up to 8 times higher than RWC values, which is the opposite compared to mass normalised $OP_M$ and $ROS_M$ concentrations. This can be explained in part by the very different units ~~using~~used for normalising ~~,~~ $OP_M$ and EF, respectively. For $OP_M$, the mass of emitted particles is used to normalise OP values, whereas for EF the mass of burnt fuel is used. ~~With our current understanding we cannot explain these differences and further research on $EF_{OP}$ and $EF_{ROS}$ need to be done. Although~~ $EF_{OP}$ and $EF_{ROS}$ could be a useful metric to compare OP and ROS per kilogram of fuel to assess the relative toxicity of emissions from different combustion sources.

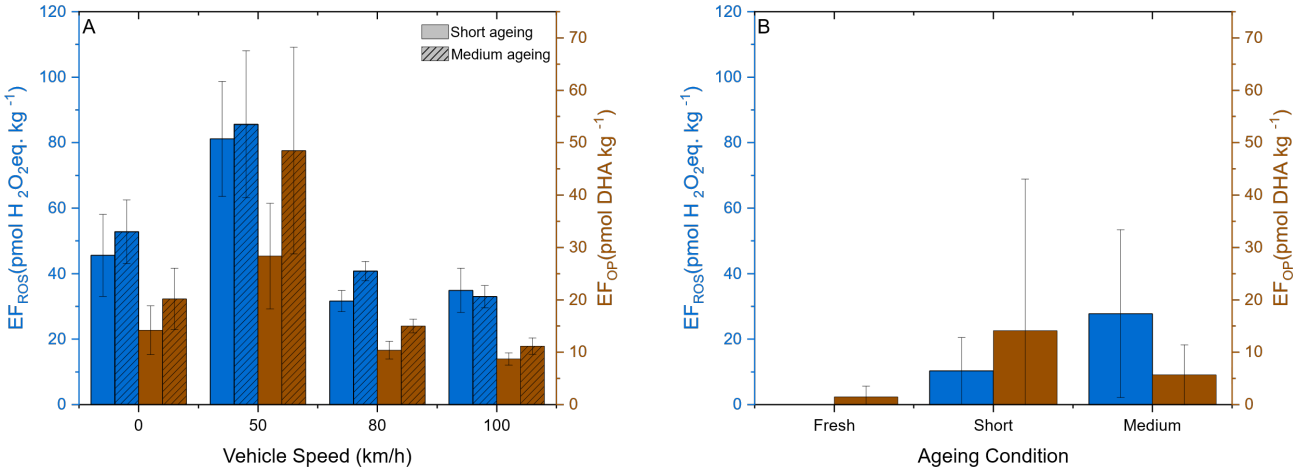


**Figure 8 Emission factors for car emissions (A) and RWC (B). The blue bars represent $EF_{ROS}$ while $EF_{OP}$ is shown in brown. The striped bars represent the medium ageing condition whereas the plain bars show short ageing. The error bars shown represent the standard deviation of the averaged values and indicate the variability of the measurements.**

## 4 Conclusion

OP and ROS concentrations of aged and fresh emissions from a gasoline car as well as wood burning stove were characterized with two online, high-time resolution instruments. On average, the RWC emissions had a up to ten times higher $OP_M$ and $ROS_M$ than the car emissions. Atmospheric ageing affects the $OP_M$ and $ROS_M$ content in particle emissions of these two sources differently: for RWC an increased $OP_M$ was observed with short ageing compared to the fresh emissions and medium aging but for car exhaust, longer ageing leads to a slightly higher $OP_M$.

In contrast, the $ROS_M$ content decreased with higher ageing for the car emissions. For the RWC emissions the opposite was observed: the $ROS_M$ concentration increased with longer ageing.

The highly dynamic changes in OP and ROS activity within one car driving cycle or wood batch, as well as the large batch-to-batch variability of values (often on time scales of a few minutes), would not be detectable with traditional offline methods. Our data indicate that the contribution of RWC emissions per µg particle emissions towards PM toxicity is significantly larger than from gasoline car emissions. However, this is also due to the implementation of a GPF, preventing most primary car emissions.

Biomass burning is the main emission source from the residential sector which can contribute more than 50% of anthropogenic $PM_{2.5}$ emissions in some parts of Europe.(Zauli-Sajani et al., 2024) The $PM_{2.5}$ mass contribution of biomass burning was shown to be as high as from traffic exhaust even at traffic sites in five European cities.(Saraga et al., 2021) Combined with the high OP and ROS activity of RWC emissions, the potential detrimental effects on human health should be considered in air quality efforts. In addition, ~~The potential significance of car emissions should be taken into consideration as well since the~~ SOA particle formation potential from car emissions with high OP and ROS activities can be~~is high~~observed, ~~although~~ even if there are almost no primary particle emissions as demonstrated in this study~~. These insights should play a major role in air quality guideline evaluations~~. Overall, the results presented here show the importance of measuring ~~air pollution~~ OP and ROS with a high-time resolution to capture their dynamic nature and to consider~~ing~~ different atmospheric ageing times of these potential PM toxicity markers.~~because they play a key role in toxicity and therefore potential health effects. add to the existing weight of evidence that OP measurements should be considered as a valid metric to evaluate the potential health effects of PM.~~

## 5 Data Availability

All data can be accessed from the corresponding author upon request.

## 6 Author Contribution

BU, AB writing – original draft preparation, investigation, methodology, formal analysis and visualization, AP, AM, C-MM, MI, PYP, MKortelainen, PM, MS, JL investigation, SJC, HC, OS, writing – reviewing & editing and conceptualization, TH, YR, RZ Resources, MKalberer writing, reviewing & editing, conceptualization, supervision and resources

## 7 Competing Interests

The authors declare that they have no conflict of interest.

## 8 Acknowledgments

We thank the SNF (Grant 192192), the Helmholtz international Laboratory aeroHEALTH (InterLabs-0005; https://aerohealth.eu) and the ULTRHAS Horizon Europe project (agreement 955390) for supporting this work and every one of the aeroHEALTH consortium that contributed to the measurement campaign.

**References**


Alves, C., Gonçalves, C., Fernandes, A. P., Tarelho, L., and Pio, C.: Fireplace and woodstove fine particle emissions from combustion of western Mediterranean wood types, Atmospheric Research, 101, 692–700, https://doi.org/10.1016/J.ATMOSRES.2011.04.015, 2011.

Atkinson, R. W., Mills, I. C., Walton, H. A., and Anderson, H. R.: Fine particle components and health—a systematic review and meta-analysis of epidemiological time series studies of daily mortality and hospital admissions, J Expo Sci Environ Epidemiol, 25, 208–214, https://doi.org/10.1038/jes.2014.63, 2015.

Bates, J. T., Fang, T., Verma, V., Zeng, L., Weber, R. J., Tolbert, P. E., Abrams, J. Y., Sarnat, S. E., Klein, M., Mulholland, J. A., and Russell, A. G.: Review of Acellular Assays of Ambient Particulate Matter Oxidative Potential: Methods and Relationships with Composition, Sources, and Health Effects, Environmental Science and Technology, 53, 4003–4019, https://doi.org/10.1021/acs.est.8b03430, 2019.

Baulig, A., Garlatti, M., Bonvallot, V., Marchand, A., Barouki, R., Marano, F., and Baeza-Squiban, A.: Involvement of reactive oxygen species in the metabolic pathways triggered by diesel exhaust particles in human airway epithelial cells, American Journal of Physiology - Lung Cellular and Molecular Physiology, 285, https://doi.org/10.1152/ajplung.00419.2002, 2003.

Brunekreef, B. and Holgate, S. T.: Air pollution and health., Lancet (London, England), 360, 1233–42, https://doi.org/10.1016/S0140-6736(02)11274-8, 2002.

Campbell, S. J., Stevanovic, S., Miljevic, B., Bottle, S. E., Ristovski, Z., and Kalberer, M.: Quantification of Particle-Bound Organic Radicals in Secondary Organic Aerosol, Environmental Science & Technology, 53, 6729–6737, https://doi.org/10.1021/acs.est.9b00825, 2019.

Campbell, S. J., Utinger, B., Barth, A., Paulson, S. E., and Kalberer, M.: Iron and Copper Alter the Oxidative Potential of Secondary Organic Aerosol: Insights from Online Measurements and Model Development, Environmental Science & Technology, https://doi.org/10.1021/ACS.EST.3C01975, 2023.

Campbell, S. J., Barth, A., Chen, G. I., Tremper, A. H., Priestman, M., Ek, D., Gu, S., Kelly, F. J., Kalberer, M., and Green, D. C.: High time resolution quantification of PM2.5 oxidative potential at a Central London roadside supersite, Environment International, 193, 109102, https://doi.org/10.1016/j.envint.2024.109102, 2024.

Charrier, J. G. and Anastasio, C.: On dithiothreitol (DTT) as a measure of oxidative potential for ambient particles: Evidence for the importance of soluble transition metals, Atmospheric Chemistry and Physics, 12, 9321–9333, https://doi.org/10.5194/acp-12-9321-2012, 2012.

Daellenbach, K. R., Uzu, G., Jiang, J., Cassagnes, L.-E., Leni, Z., Vlachou, A., Stefenelli, G., Canonaco, F., Weber, S., Segers, A., Kuenen, J. J. P., Schaap, M., Favez, O., Albinet, A., Aksoyoglu, S., Dommen, J., Baltensperger, U., Geiser, M., Haddad, I. E., Jaffrezo, J.-L., Prévôt, A. S. H., El Haddad, I., Jaffrezo, J.-L., and Prévôt, A. S. H.: Sources of particulate-matter air pollution and its oxidative potential in Europe, Nature, 587, 414–419, https://doi.org/10.1038/s41586-020-2902-8, 2020.

Donaldson, K., Stone, V., Seaton, A., and MacNee, W.: Ambient particle inhalation and the cardiovascular system: Potential mechanisms, Environmental Health Perspectives, 109, 523–527, https://doi.org/10.1289/ehp.01109s4523, 2001.

Epstein, S. A., Blair, S. L., and Nizkorodov, S. A.: Direct Photolysis of α-Pinene Ozonolysis Secondary Organic Aerosol: Effect on Particle Mass and Peroxide Content, Environ. Sci. Technol., 48, 11251–11258, https://doi.org/10.1021/es502350u, 2014.

Erlandsson, L., Lindgren, R., Nääv, Å., Krais, A. M., Strandberg, B., Lundh, T., Boman, C., Isaxon, C., Hansson, S. R., and Malmqvist, E.: Exposure to wood smoke particles leads to inflammation, disrupted proliferation and damage to cellular structures in a human first trimester trophoblast cell line, Environmental Pollution, 264, 114790, https://doi.org/10.1016/J.ENVPOL.2020.114790, 2020.

European Parliament: Ambient air quality and cleaner air for Europe. Recast, 2024.

European Union: Proposal for a Directive of the European Parliament and of the Council on ambient air quality and cleaner air for Europe (recast), 2022.

Fang, Z., Lai, A., Dongmei Cai, Chunlin Li, Carmieli, R., Chen, J., Wang, X., and Rudich, Y.: Secondary Organic Aerosol Generated from Biomass Burning Emitted Phenolic Compounds: Oxidative Potential, Reactive Oxygen Species, and Cytotoxicity, Environ. Sci. Technol., 58, 8194–8206, https://doi.org/10.1021/acs.est.3c09903, 2024.

Gao, J., Chen, H., Liu, Y., Laurikko, J., Li, Y., Li, T., and Tu, R.: Comparison of NOx and PN emissions between Euro 6 petrol and diesel passenger cars under real-world driving conditions, Science of The Total Environment, 801, 149789, https://doi.org/10.1016/j.scitotenv.2021.149789, 2021.

Gon, H. D. V. D., Bergström, R., Fountoukis, C., Johansson, C., Pandis, S., Simpson, D., and Visschedijk, A.: Particulate emissions from residential wood combustion in Europe - revised estimates and an evaluation, Atmospheric Chemistry and Physics, 15, 6503–6519, https://doi.org/10.5194/ACP-15-6503-2015, 2014.

Gonçalves, C., Alves, C., Evtyugina, M., Mirante, F., Pio, C., Caseiro, A., Schmidl, C., Bauer, H., and Carvalho, F.: Characterisation of PM10 emissions from woodstove combustion of common woods grown in Portugal, Atmospheric Environment, 44, 4474–4480, https://doi.org/10.1016/J.ATMOSENV.2010.07.026, 2010.

Guascito, M. R., Lionetto, M. G., Mazzotta, F., Conte, M., Giordano, M. E., Caricato, R., De Bartolomeo, A. R., Dinoi, A., Cesari, D., Merico, E., Mazzotta, L., and Contini, D.: Characterisation of the correlations between oxidative potential and in vitro biological effects of PM10 at three sites in the central Mediterranean, Journal of Hazardous Materials, 448, 130872, https://doi.org/10.1016/j.jhazmat.2023.130872, 2023.

Hart, J. E., Liao, X., Hong, B., Puett, R. C., Yanosky, J. D., Suh, H., Kioumourtzoglou, M. A., Spiegelman, D., and Laden, F.: The association of long-term exposure to PM2.5 on all-cause mortality in the Nurses' Health Study and the impact of measurement-error correction, Environmental Health, 14, 38, https://doi.org/10.1186/s12940-015-0027-6, 2015.

Hartikainen, A. H., Ihalainen, M., Yli-Pirilä, P., Hao, L., Kortelainen, M., Pieber, S. M., and Sippula, O.: Photochemical transformation and secondary aerosol formation potential of Euro6 gasoline and diesel passenger car exhaust emissions, Journal of Aerosol Science, 171, 106159, https://doi.org/10.1016/j.jaerosci.2023.106159, 2023.

Heo, J., Schauer, J. J., Yi, O., Paek, D., Kim, H., and Yi, S.-M.: Fine Particle Air Pollution and Mortality: Importance of Specific Sources and Chemical Species, Epidemiology, 25, 379–388, https://doi.org/10.1097/EDE.0000000000000044, 2014.

Heringa, M. F., DeCarlo, P. F., Chirico, R., Lauber, A., Doberer, A., Good, J., Nussbaumer, T., Keller, A., Burtscher, H., Richard, A., Miljevic, B., Prevot, A. S. H., and Baltensperger, U.: Time-Resolved Characterization of Primary Emissions from Residential Wood Combustion Appliances, Environmental Science & Technology, 46, 11418–11425, https://doi.org/10.1021/es301654w, 2012.

Ihalainen, M., Tiitta, P., Czech, H., Yli-Pirilä, P., Hartikainen, A., Kortelainen, M., Tissari, J., Stengel, B., Sklorz, M., Suhonen, H., Lamberg, H., Leskinen, A., Kiendler-Scharr, A., Harndorf, H., Zimmermann, R., Jokiniemi, J., and Sippula, O.: A novel

high-volume Photochemical Emission Aging flow tube Reactor (PEAR), Aerosol Science and Technology, 53, 276–294, https://doi.org/10.1080/02786826.2018.1559918/SUPPL_FILE/UAST_A_1559918_SM0097.DOCX, 2019.

Ihantola, T., Hirvonen, M.-R., Ihalainen, M., Hakkarainen, H., Sippula, O., Tissari, J., Bauer, S., Di Bucchianico, S., Rastak, N., Hartikainen, A., Leskinen, J., Yli-Pirilä, P., Martikainen, M.-V., Miettinen, M., Suhonen, H., Rönkkö, T. J., Kortelainen, M., Lamberg, H., Czech, H., Martens, P., Orasche, J., Michalke, B., Yildirim, A. Ö., Jokiniemi, J., Zimmermann, R., and Jalava, P. I.: Genotoxic and inflammatory effects of spruce and brown coal briquettes combustion aerosols on lung cells at the air-liquid interface, Science of The Total Environment, 806, 150489, https://doi.org/10.1016/j.scitotenv.2021.150489, 2022.

Jiang, H. and Jang, M.: Dynamic Oxidative Potential of Atmospheric Organic Aerosol under Ambient Sunlight, Environmental Science and Technology, 52, 7496–7504, https://doi.org/10.1021/acs.est.8b00148, 2018.

Kelly, F. J.: Oxidative stress: its role in air pollution and adverse health effects, Occup Environ Med, 60, 612–616, https://doi.org/10.1136/oem.60.8.612, 2003.

Kelly, F. J. and Fussell, J. C.: Size, source and chemical composition as determinants of toxicity attributable to ambient particulate matter, Atmospheric Environment, 60, 504–526, https://doi.org/10.1016/j.atmosenv.2012.06.039, 2012.

Khan, M. R.: Immobilized enzymes: a comprehensive review, Bulletin of the National Research Centre, 45, 207, https://doi.org/10.1186/s42269-021-00649-0, 2021.

Kjällstrand, J. and Petersson, G.: Phenolic antioxidants in wood smoke, Science of The Total Environment, 277, 69–75, https://doi.org/10.1016/S0048-9697(00)00863-9, 2001.

Künzi, L., Krapf, M., Daher, N., Dommen, J., Jeannet, N., Schneider, S., Platt, S., Slowik, J. G., Baumlin, N., Salathe, M., Prévôt, A. S. H., Kalberer, M., Strähl, C., Dümbgen, L., Sioutas, C., Baltensperger, U., and Geiser, M.: Toxicity of aged gasoline exhaust particles to normal and diseased airway epithelia, Scientific Reports, 5, 1–10, https://doi.org/10.1038/srep11801, 2015.

Laden, F., Schwartz, J., Speizer, F. E., and Dockery, D. W.: Reduction in fine particulate air pollution and mortality: Extended follow-up of the Harvard Six Cities Study, American Journal of Respiratory and Critical Care Medicine, 173, 667–672, https://doi.org/10.1164/rccm.200503-443OC, 2006.

Lepeule, J., Laden, F., Dockery, D., and Schwartz, J.: Chronic exposure to fine particles and mortality: An extended follow-up of the Harvard six cities study from 1974 to 2009, Environmental Health Perspectives, 120, 965–970, https://doi.org/10.1289/ehp.1104660, 2012.

Leskinen, J., Hartikainen, A., Väätäinen, S., Ihalainen, M., Virkkula, A., Mesceriakovas, A., Tiitta, P., Miettinen, M., Lamberg, H., Czech, H., Yli-Pirilä, P., Tissari, J., Jakobi, G., Zimmermann, R., and Sippula, O.: Photochemical Aging Induces Changes in the Effective Densities, Morphologies, and Optical Properties of Combustion Aerosol Particles, Environ. Sci. Technol., 57, 5137–5148, https://doi.org/10.1021/acs.est.2c04151, 2023.

Li, J., Li, J., Wang, G., Ho, K. F., Dai, W., Zhang, T., Wang, Q., Wu, C., Li, L., Li, L., and Zhang, Q.: Effects of atmospheric aging processes on in vitro induced oxidative stress and chemical composition of biomass burning aerosols, Journal of Hazardous Materials, 401, 123750, https://doi.org/10.1016/J.JHAZMAT.2020.123750, 2021.

Li, N., Hao, M., Phalen, R. F., Hinds, W. C., and Nel, A. E.: Particulate air pollutants and asthma: A paradigm for the role of oxidative stress in PM-induced adverse health effects, Clinical Immunology, 109, 250–265, https://doi.org/10.1016/j.clim.2003.08.006, 2003.

Martens, P., Czech, H., Tissari, J., Ihalainen, M., Suhonen, H., Sklorz, M., Jokiniemi, J., Sippula, O., and Zimmermann, R.: Emissions of Gases and Volatile Organic Compounds from Residential Heating: A Comparison of Brown Coal Briquettes and Logwood Combustion, Energy Fuels, 35, 14010–14022, https://doi.org/10.1021/acs.energyfuels.1c01667, 2021.

Mukherjee, A., Hartikainen, A., Joutsensaari, J., Basnet, S., Mesceriakovas, A., Ihalainen, M., Yli-Pirilä, P., Leskinen, J., Somero, M., Louhisalmi, J., Fang, Z., Kalberer, M., Rudich, Y., Tissari, J., Czech, H., Zimmermann, R., and Sippula, O.: Black carbon and particle lung-deposited surface area in residential wood combustion emissions: Effects of an electrostatic precipitator and photochemical aging, Science of The Total Environment, 952, 175840, https://doi.org/10.1016/j.scitotenv.2024.175840, 2024.

Njus, D., Asmaro, K., Li, G., and Palomino, E.: Redox cycling of quinones reduced by ascorbic acid, Chemico-Biological Interactions, 373, 110397, https://doi.org/10.1016/J.CBI.2023.110397, 2023.

Nordin, E. Z., Uski, O., Nyström, R., Jalava, P., Eriksson, A. C., Genberg, J., Roldin, P., Bergvall, C., Westerholm, R., Jokiniemi, J., Pagels, J. H., Boman, C., and Hirvonen, M. R.: Influence of ozone initiated processing on the toxicity of aerosol particles from small scale wood combustion, Atmospheric Environment, 102, 282–289, https://doi.org/10.1016/J.ATMOSENV.2014.11.068, 2015.

Offer, S., Hartner, E., Di Bucchianico, S., Bisig, C., Bauer, S., Pantzke, J., Zimmermann, E. J., Cao, X., Binder, S., Kuhn, E., Huber, A., Jeong, S., Käfer, U., Martens, P., Mesceriakovas, A., Bendl, J., Brejcha, R., Buchholz, A., Gat, D., Hohaus, T., Rastak, N., Jakobi, G., Kalberer, M., Kanashova, T., Hu, Y., Ogris, C., Marsico, A., Theis, F., Pardo, M., Gröger, T., Oeder, S., Orasche, J., Paul, A., Ziehm, T., Zhang, Z.-H. H., Adam, T., Sippula, O., Sklorz, M., Schnelle-Kreis, J., Czech, H., Kiendler-Scharr, A., Rudich, Y., and Zimmermann, R.: Effect of Atmospheric Aging on Soot Particle Toxicity in Lung Cell Models at the Air-Liquid Interface: Differential Toxicological Impacts of Biogenic and Anthropogenic Secondary Organic Aerosols (SOAs), Environmental health perspectives, 130, 1–19, https://doi.org/10.1289/EHP9413, 2022.

Orru, H., Olstrup, H., Kukkonen, J., López-Aparicio, S., Segersson, D., Geels, C., Tamm, T., Riikonen, K., Maragkidou, A., Sigsgaard, T., Brandt, J., Grythe, H., and Forsberg, B.: Health impacts of PM2.5 originating from residential wood combustion in four nordic cities, BMC Public Health, 22, 1–13, https://doi.org/10.1186/S12889-022-13622-X/FIGURES/3, 2022.

Øvrevik, J., Refsnes, M., Låg, M., Holme, J. A., and Schwarze, P. E.: Activation of Proinflammatory Responses in Cells of the Airway Mucosa by Particulate Matter: Oxidant- and Non-Oxidant-Mediated Triggering Mechanisms, Biomolecules, 5, 1399–1440, https://doi.org/10.3390/biom5031399, 2015.

Paul, A., Fang, Z., Martens, P., Mukherjee, A., Jakobi, G., Ihalainen, M., Kortelainen, M., Somero, M., Yli-Pirilä, P., Hohaus, T., Czech, H., Kalberer, M., Sippula, O., Rudich, Y., Zimmermann, R., and Kiendler-Scharr, A.: Formation of secondary aerosol from emissions of a Euro 6d-compliant gasoline vehicle with particle filter, Environ. Sci.: Atmos., 10.1039.D3EA00165B, https://doi.org/10.1039/D3EA00165B, 2024.

Pizzino, G., Irrera, N., Cucinotta, M., Pallio, G., Mannino, F., Arcoraci, V., Squadrito, F., Altavilla, D., and Bitto, A.: Oxidative Stress: Harms and Benefits for Human Health, https://doi.org/10.1155/2017/8416763, 2017.

Platt, S. M., Haddad, I. El., Pieber, S. M., Huang, R.-J., Zardini, A. A., Clairotte, M., Suarez-Bertoa, R., Barmet, P., Pfaffenberger, L., Wolf, R., Slowik, J. G., Fuller, S. J., Kalberer, M., Chirico, R., Dommen, J., Astorga, C., Zimmermann, R., Marchand, N., Hellebust, S., Temime-Roussel, B., Baltensperger, U., and Prévôt, A. S. H.: Two-stroke scooters are a dominant source of air pollution in many cities, Nature Communications, 5, 3749, https://doi.org/10.1038/ncomms4749, 2014.

Platt, S. M., El Haddad, I., Pieber, S. M., Zardini, A. A., Suarez-Bertoa, R., Clairotte, M., Daellenbach, K. R., Huang, R.-J., Slowik, J. G., Hellebust, S., Temime-Roussel, B., Marchand, N., De Gouw, J., Jimenez, J. L., Hayes, P. L., Robinson, A. L.,

Baltensperger, U., Astorga, C., and Prévôt, A. S. H.: Gasoline cars produce more carbonaceous particulate matter than modern filter-equipped diesel cars, Sci Rep, 7, 4926, https://doi.org/10.1038/s41598-017-03714-9, 2017.

Prahalad, A. K., Inmon, J., Dailey, L. A., Madden, M. C., Ghio, A. J., and Gallagher, J. E.: Air pollution particles mediated oxidative DNA base damage in a cell free system and in human airway epithelial cells in relation to particulate metal content and bioreactivity, Chemical Research in Toxicology, 14, 879–887, https://doi.org/10.1021/tx010022e, 2001.

Reda, A. A., Czech, H., Schnelle-Kreis, J., Sippula, O., Orasche, J., Weggler, B., Abbaszade, G., Arteaga-Salas, J. M., Kortelainen, M., Tissari, J., Jokiniemi, J., Streibel, T., and Zimmermann, R.: Analysis of gas-phase carbonyl compounds in emissions from modern wood combustion appliances: Influence of wood type and combustion appliance, Energy and Fuels, 29, 3897–3907, https://doi.org/10.1021/EF502877C/SUPPL_FILE/EF502877C_SI_002.PDF, 2015.

Saraga, D., Maggos, T., Degrendele, C., Klánová, J., Horvat, M., Kocman, D., Kanduč, T., Garcia Dos Santos, S., Franco, R., Gómez, P. M., Manousakas, M., Bairachtari, K., Eleftheriadis, K., Kermenidou, M., Karakitsios, S., Gotti, A., and Sarigiannis, D.: Multi-city comparative PM2.5 source apportionment for fifteen sites in Europe: The ICARUS project, Science of The Total Environment, 751, 141855, https://doi.org/10.1016/J.SCITOTENV.2020.141855, 2021.

Schneider, E., Czech, H., Hartikainen, A., Hansen, H. J., Gawlitta, N., Ihalainen, M., Yli-Pirilä, P., Somero, M., Kortelainen, M., Louhisalmi, J., Orasche, J., Fang, Z., Rudich, Y., Sippula, O., Rüger, C. P., and Zimmermann, R.: Molecular composition of fresh and aged aerosols from residential wood combustion and gasoline car with modern emission mitigation technology, Environ. Sci.: Processes Impacts, 10.1039.D4EM00106K, https://doi.org/10.1039/D4EM00106K, 2024.

Steimer, S. S., Delvaux, A., Campbell, S. J., Gallimore, P. J., Grice, P., Howe, D. J., Pitton, D., Claeys, M., Hoffmann, T., and Kalberer, M.: Synthesis and characterisation of peroxypinic acids as proxies for highly oxygenated molecules (HOMs) in secondary organic aerosol, Atmospheric Chemistry and Physics, 18, 10973–10983, https://doi.org/10.5194/acp-18-10973-2018, 2018.

Uski, O., Jalava, P. I., Happo, M. S., Torvela, T., Leskinen, J., Mäki-Paakkanen, J., Tissari, J., Sippula, O., Lamberg, H., Jokiniemi, J., and Hirvonen, M.-R.: Effect of fuel zinc content on toxicological responses of particulate matter from pellet combustion in vitro, Science of The Total Environment, 511, 331–340, https://doi.org/10.1016/j.scitotenv.2014.12.061, 2015.

Utinger, B., Campbell, S. J., Bukowiecki, N., Barth, A., Gfeller, B., Freshwater, R., Rüegg, H.-R., and Kalberer, M.: An automated online field instrument to quantify the oxidative potential of aerosol particles via ascorbic acid oxidation, Atmospheric Measurement Techniques, 16, 2641–2654, https://doi.org/10.5194/amt-16-2641-2023, 2023.

Vicente, E. D., Duarte, M. A., Calvo, A. I., Nunes, T. F., Tarelho, L., and Alves, C. A.: Emission of carbon monoxide, total hydrocarbons and particulate matter during wood combustion in a stove operating under distinct conditions, Fuel Processing Technology, 131, 182–192, https://doi.org/10.1016/J.FUPROC.2014.11.021, 2015.

Walgraeve, C., Demeestere, K., Dewulf, J., Zimmermann, R., and Van Langenhove, H.: Oxygenated polycyclic aromatic hydrocarbons in atmospheric particulate matter: Molecular characterization and occurrence, Atmospheric Environment, 44, 1831–1846, https://doi.org/10.1016/J.ATMOSENV.2009.12.004, 2010.

Wang, S., Gallimore, P. J., Liu-Kang, C., Yeung, K., Campbell, S. J., Utinger, B., Liu, T., Peng, H., Kalberer, M., Chan, A. W. H., and Abbatt, J. P. D.: Dynamic Wood Smoke Aerosol Toxicity during Oxidative Atmospheric Aging, Environmental Science and Technology, 57, 1246–1256, https://doi.org/10.1021/ACS.EST.2C05929/ASSET/IMAGES/LARGE/ES2C05929_0006.JPEG, 2023.

Wong, J. P. S., Tsagkaraki, M., Tsiodra, I., Mihalopoulos, N., Violaki, K., Kanakidou, M., Sciare, J., Nenes, A., and Weber, R. J.: Effects of Atmospheric Processing on the Oxidative Potential of Biomass Burning Organic Aerosols, Environmental Science and Technology, 53, 6747–6756, https://doi.org/10.1021/acs.est.9b01034, 2019.

World Health Organization: WHO global air quality guidelines. Particulate matter (PM2.5 and PM10), ozone, nitrogen dioxide, sulfur dioxide and carbon monoxide., 2021.

Wragg, F. P. H., Fuller, S. J., Freshwater, R., Green, D. C., Kelly, F. J., and Kalberer, M.: An automated online instrument to quantify aerosol-bound reactive oxygen species (ROS) for ambient measurement and health-relevant aerosol studies, Atmospheric Measurement Techniques, 9, 4891–4900, https://doi.org/10.5194/amt-9-4891-2016, 2016.

Zauli-Sajani, S., Thunis, P., Pisoni, E., Bessagnet, B., Monforti-Ferrario, F., De Meij, A., Pekar, F., and Vignati, E.: Reducing biomass burning is key to decrease PM2.5 exposure in European cities, Sci Rep, 14, 10210, https://doi.org/10.1038/s41598-024-60946-2, 2024.

Zhang, Z.-H. H., Hartner, E., Utinger, B., Gfeller, B., Paul, A., Sklorz, M., Czech, H., Yang, B. X., Su, X. Y., Jakobi, G., Orasche, J., Schnelle-Kreis, J., Jeong, S., Gröger, T., Pardo, M., Hohaus, T., Adam, T., Kiendler-Scharr, A., Rudich, Y., Zimmermann, R., and Kalberer, M.: Are reactive oxygen species (ROS) a suitable metric to predict toxicity of carbonaceous aerosol particles?, Atmospheric Chemistry and Physics Discussions, 22, 1–29, https://doi.org/10.5194/acp-2021-666, 2021.

Zhao, J., Zhang, Y., Sisler, J. D., Shaffer, J., Leonard, S. S., Morris, A. M., Qian, Y., Bello, D., and Demokritou, P.: Assessment of reactive oxygen species generated by electronic cigarettes using acellular and cellular approaches, Journal of Hazardous Materials, 344, 549–557, https://doi.org/10.1016/j.jhazmat.2017.10.057, 2018.

**Supplement Information**

Particle losses were characterized in a separate set of experiments using SOA produced via dark ozonolysis in a flow tube reactor. SOA was generated by passing 0.3 l/min of synthetic air over a heart-shaped flask filled with α-pinene. This flow was mixed with 4.7 l/min coming from an ozone-generating UV lamp (UVP LLC) into a 2.5 l glass flow tube. After the flow tube a dilution flow of 12 l/min was added. Similar particle mass and number concentrations as well as flow rates through the denuders were recreated as present during the emission measurements. By comparing the particle number size distributions measured with a scanning mobility particle sizer (TSI) before and after the denuders, the particle losses were determined to be approximately 10%

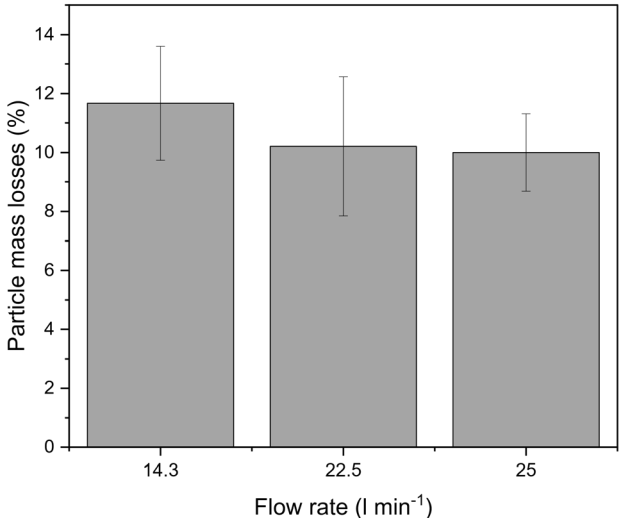


*Figure S 1: Particle loss caused by the charcoal denuders at different flow rates*

~~Activated charcoal was added to the DCFH assay to simulate the high surface area of soot in order to test the hypothesis that the high concentrations in the RWC experiments might cause the HRP enzyme activity to be reduced below blank levels. To get the smallest possible particle size, the charcoal was ground in a mortar. It was then suspended in water and thoroughly mixed to produce a homogenous mixture. For a more controlled environment we used an offline approach as described in Campbell et al., 2021.(Campbell et al., 2021) In order to better align the protocol with the online method of the OPROSI, some adjustments were made. In this revised protocol, soot is added to the HRP and allowed to react for 9 minutes. After this, the mixture is passed through a syringe filter to remove the insoluble particles. Subsequently, DCFH is added and the sample is incubated for an additional 9 minutes. Figure S 2 shows that the addition of charcoal reduced the response of the assay below the blank. This could be an indicator that the negative signals from the OPROSI during primary RWC experiments are caused by the physical presence of insoluble particles in the instrument.~~

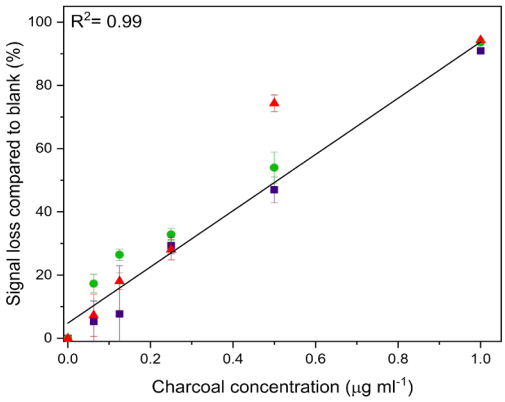


*Figure S 2 Soot measurements in triplicates to show the sensitivity loss in %. Error bars are standard deviation of triplicate measurements.*

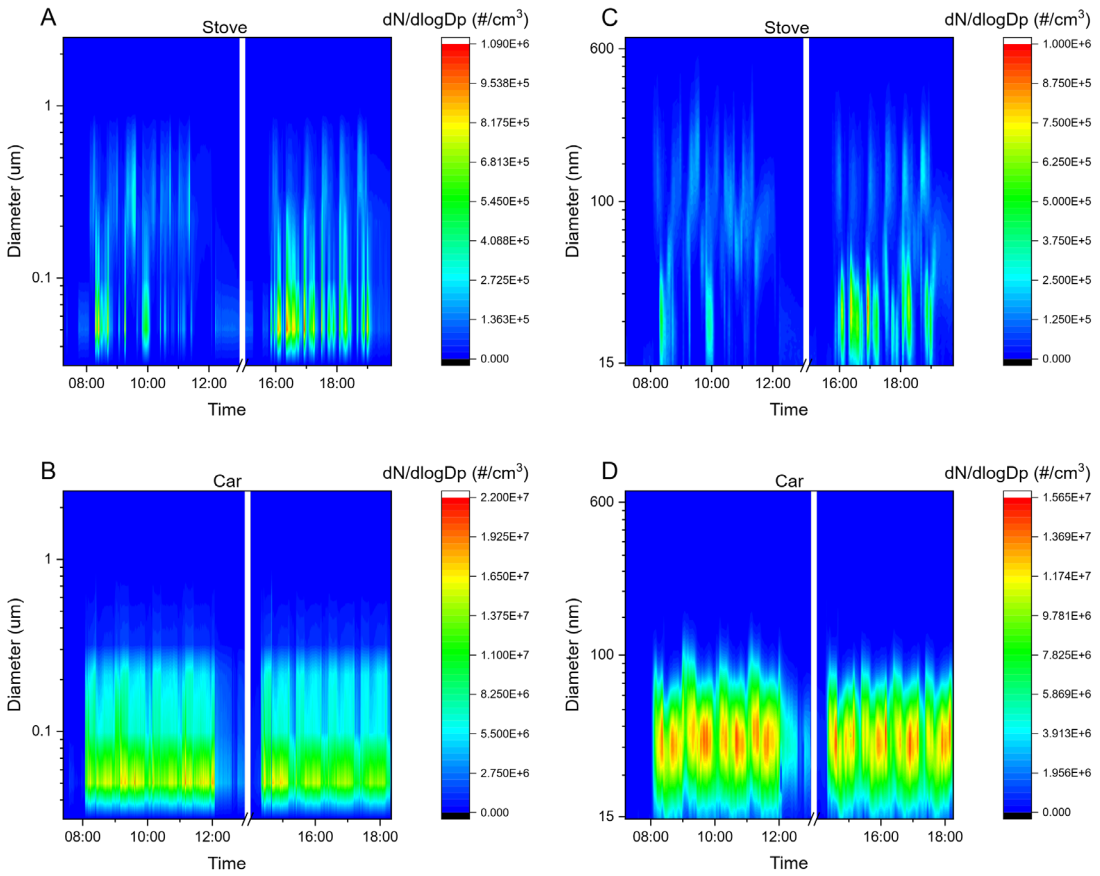


*Figure S 2~~3~~: ELPI contour plots of particle numbers for one stove (A) and one car (B) experiment. No significant particle number concentrations were measured in higher size bins. Equivalent SMPS contour plots of the same stove (C) and car (D) measurements show the absence of particles above 600 nm for stove and above 200nm for car emissions, respectively.*

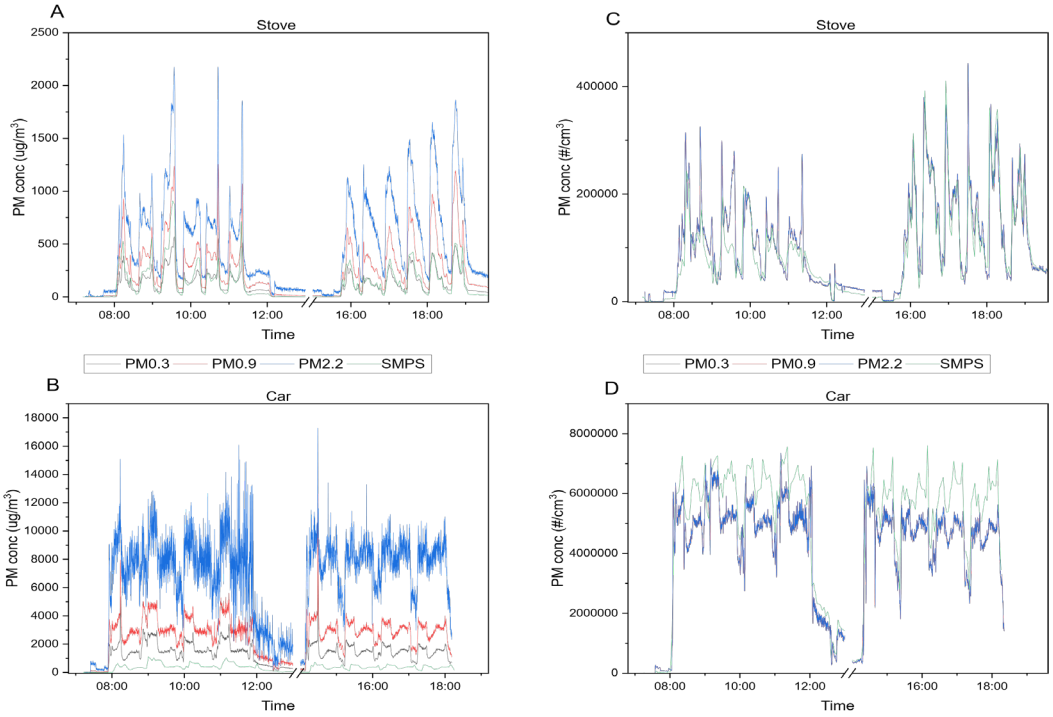


*Figure S 1: Mass concentrations measured by the SMPS and ELPI during a stove (A) and car (B) exhaust measurement. The ELPI results are shown for three size ranges. Number concentrations measured by the SMPS and ELPI during a stove (C) and car (D) measurement. The ELPI results are shown for three size ranges. Nearly no number concentration differences between the different size ranges of the ELPI are visible. However, large differences in mass concentrations were caused by few artefact particles in larger size bins.*

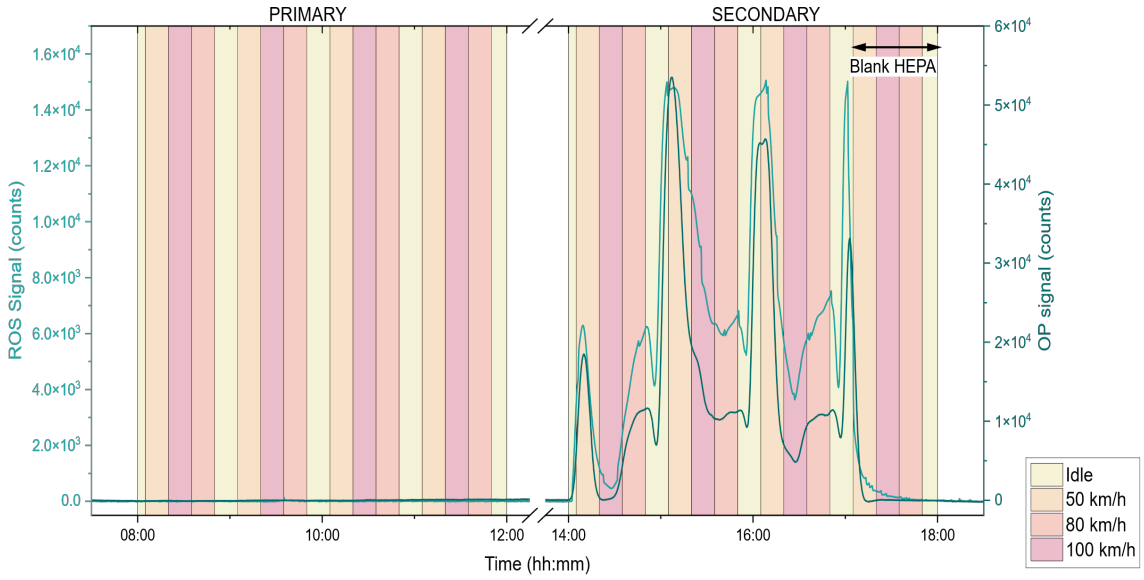


*Figure S 4: Blank-corrected signal intensities of OP and ROS activity of primary and secondary car emissions over eight hours. The different coloured time periods correspond to the driving cycle conditions of the driving cycle. The last hour of each experiment was used as a HEPA blank measurement. No OP and ROS signal was observed for primary exhaust and no gas-phase artefacts were observed.*

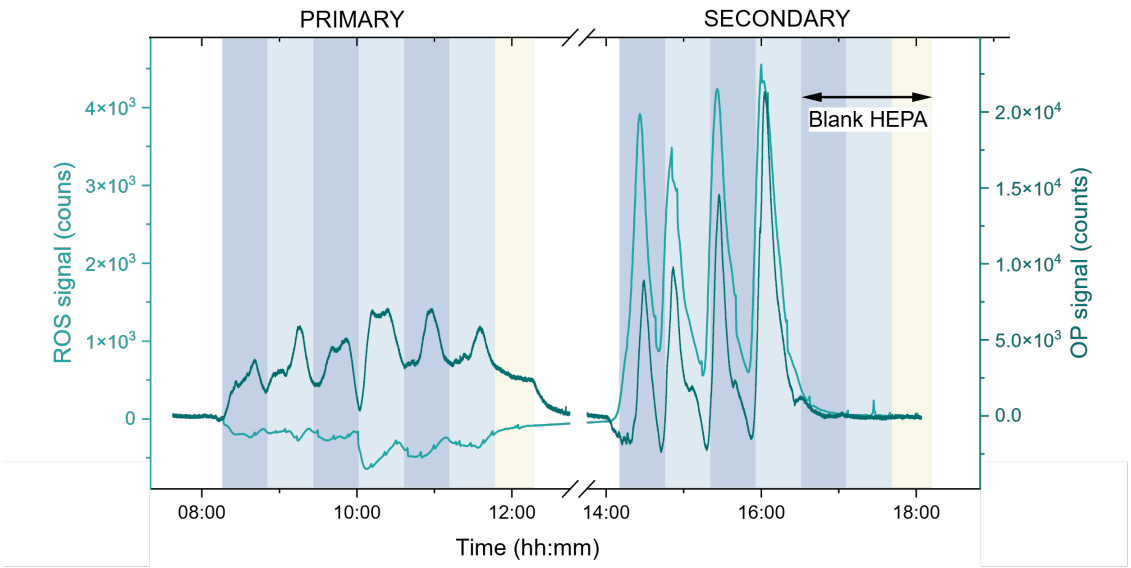


*Figure S 5: Blank-corrected signal intensities of OP and ROS activity in primary (left) and secondary (right) RWC emission particles. The colours indicate the addition of a new batch of wood. In total, OP and ROS content were measured in primary and secondary emissions of each six batches of wood. The last batch during primary emissions was left to reach an ember phase (yellow stripes). The last two batches including the ember phase were used as a blank measurement during the secondary emissions.*

Activated charcoal was added to the DCFH assay to simulate the high surface area of soot in order to test the hypothesis that the high concentrations in the RWC experiments might cause the HRP enzyme activity to be reduced below blank levels. To get the smallest possible particle size, the charcoal was ground in a mortar. It was then suspended in water and thoroughly mixed to produce a homogenous mixture. For a more controlled environment we used an offline approach as described in Campbell et al., 2021.(Campbell et al., 2021) In order to better align the protocol with the online method of the OPROSI, some adjustments were made. In this revised protocol, soot is added to the HRP and allowed to react for 9 minutes. After this, the mixture is passed through a syringe filter to remove the insoluble particles. Subsequently, DCFH is added and the sample is incubated for an additional 9 minutes. Figure S 2 shows that the addition of charcoal reduced the response of the assay below the blank. This could be an indicator that the negative signals from the OPROSI during primary RWC experiments are caused by the physical presence of insoluble particles in the instrument.

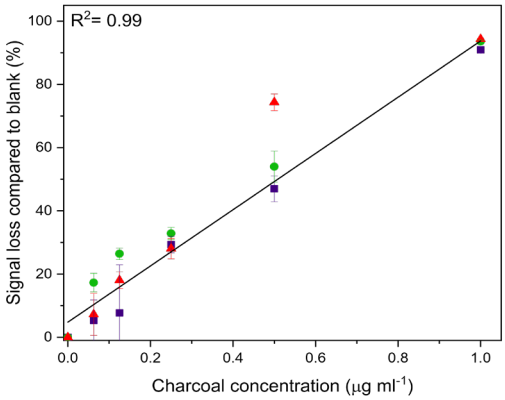


*Figure S ~~6~~2 Soot measurements in triplicates to show the sensitivity loss in %. Error bars are standard deviation of triplicate measurements.*

**References**

Campbell, S. J., Wolfer, K., Utinger, B., Westwood, J., Zhang, Z.-H., Bukowiecki, N., Steimer, S. S., Vu, T. V., Xu, J., Straw, N., Thomson, S., Elzein, A., Sun, Y., Liu, D., Li, L., Fu, P., Lewis, A. C., Harrison, R. M., Bloss, W. J., Loh, M., Miller, M. R., Shi, Z., and Kalberer, M.: Atmospheric conditions and composition that influence PM 2.5 oxidative potential in Beijing, China, Atmos. Chem. Phys, 21, 5549–5573, https://doi.org/10.5194/acp-21-5549-2021, 2021.